Kinetic Study of the Reactions of Cl Atoms with $CF_3CH_2CH_2OH$, $CF_3CF_2CH_2OH$, $CHF_2CF_2CH_2OH$, and $CF_3CHFCF_2CH_2OH$

Vassileios C. Papadimitriou,[†] Dimitrios K. Papanastasiou, Vassileios G. Stefanopoulos, Aristotelis M. Zaras, Yannis G. Lazarou,[‡] and Panos Papagiannakopoulos*

Laboratory of Photochemistry and Kinetics, Department of Chemistry, University of Crete, 71003 Heraklion, Crete, Greece

Received: June 18, 2007; In Final Form: August 20, 2007

The reaction kinetics of chlorine atoms with a series of partially fluorinated straight-chain alcohols, $CF_3CH_2CH_2OH$ (**1**), $CF_3CF_2CH_2OH$ (**2**), $CHF_2CF_2CH_2OH$ (**3**), and $CF_3CHFCF_2CH_2OH$ (**4**), were studied in the gas phase over the temperature range of 273−363 K by using very low-pressure reactor mass spectrometry. The absolute rate coefficients were given by the expressions (in cm^3 $molecule^{-1}$ s^{-1}): $k_1 = (4.42 \pm 0.48) \times 10^{-11}$ exp(−255 ± 20/T); $k_1(303) = (1.90 \pm 0.17) \times 10^{-11}$, $k_2 = (2.23 \pm 0.31) \times 10^{-11}$ exp(−1065 ± 106/T); $k_2(303) = (6.78 \pm 0.63) \times 10^{-13}$, $k_3 = (8.51 \pm 0.62) \times 10^{-12}$ exp(−681 ± 72/*T*); $k_3(303) = (9.00 \pm 0.82) \times 10^{-13}$ and $k_4 = (6.18 \pm 0.84) \times 10^{-12}$ exp(−736 ± 42/*T*); $k_4(303) = (5.36 \pm 0.51) \times 10^{-13}$. The quoted 2σ uncertainties include the systematic errors. All title reactions proceed via a hydrogen atom metathesis mechanism leading to HCl. Moreover, the oxidation of the primarily produced radicals was investigated, and the end products were the corresponding aldehydes (R_F−CHO; R_F = $-CH_2CF_3$, $-CF_2CF_3$, $-CF_2CHF_2$, and $-CF_2CHFCF_3$), providing a strong experimental indication that the primary reactions proceed mainly via the abstraction of a methylenic hydrogen adjacent to a hydroxyl group. Finally, the bond strengths and ionization potentials for the title compounds were determined by density functional theory calculations, which also suggest that the α-methylenic hydrogen is mainly under abstraction by Cl atoms. The correlation of room-temperature rate coefficients with ionization potentials for a set of 27 molecules, comprising fluorinated C2−C5 ethers and C2−C4 alcohols, is good with an average deviation of a factor of 2, and is given by the expression log(*k*) (in cm^3 $molecule^{-1}$ s^{-1}) = (5.8 ± 1.4) − (1.56 ± 0.13) × (ionization potential (in eV)).

1. Introduction

The negative impact of chlorofluorocarbons (CFCs) and hydrochlorofluorocarbons (HCFCs) in stratospheric ozone depletion[1,2] and global warming[1] has led to international agreements (Montreal Protocol), which have imposed restrictions on their production and have stressed the need for their replacement with more friendly compounds. In particular, hydrofluorocarbons (HFCs) have been suggested as potential substitutes because they do not contain chlorine or bromine atoms and therefore have no contribution to the stratospheric ozone destruction.[3] However, their strong infrared absorbance in the atmospheric window, due to the C−F bonds, and their relatively long atmospheric lifetimes classify them among the anthropogenic greenhouse gases,[1] which are regulated by the Kyoto Protocol, and therefore need to be replaced by environmentally friendly alternatives.

Partially fluorinated alcohols (HFAs) are considered among the most promising CFC substitutes because they are expected to have higher chemical reactivities than HFCs due to the presence of the −OH group and therefore shorter atmospheric lifetimes. HFAs are already used as cleaning agents[4] as well as in a variety of industrial applications[5], and therefore it is essential to assess their impact on global warming and climate change. At first it is very important to determine their atmospheric lifetimes by measuring their rate coefficients with major atmospheric reactants, such as OH radicals and Cl atoms, which initiate their chemical degradation in the troposphere. Although the reaction with OH radicals is the main removal pathway of HFAs in the troposphere, the reactions with less abundant Cl atoms may also contribute to their removal due to the higher reactivity of Cl atoms. Concentrations of chlorine atoms on the order of 10^4 molecule cm^{-3} have been detected over the marine boundary layer[6−9] as well as during ozone episodes in urban atmospheres.[10] Moreover, the reaction kinetics of HFAs with chlorine atoms will provide (a) information about the relationship between structure (position and degree of fluorination) and chemical reactivity of HFAs and (b) comparison with the reactivity of other CFC alternatives. In addition, it will provide information about the primary reaction pathways of HFAs, and therefore about the degradation mechanism of HFAs in the troposphere. Reaction kinetics of several HFAs with Cl atoms have been studied in the past by three groups,[11−14] in addition to the study of their tropospheric degradation mechanisms.

The aim of this work is to measure the absolute rate coefficients for reactions 1−4 over the temperature range of 273−363 K by employing the very low-pressure reactor mass spectrometry (VLPR-MS). Furthermore, the subsequent oxidation mechanism was also investigated by mass spectrometric end-product analysis.

* Author to whom correspondence should be addressed. E-mail: panosp@chemistry.uoc.gr.

[†] Present address: Earth System Research Laboratory, National Oceanic and Atmospheric Administration, 325 Broadway, Boulder, CO 80305-3328.

[‡] Present address: Institute of Physical Chemistry, National Centre for Scientific Research "Demokritos", Aghia Paraskevi 153 10, Attiki, Greece.

10.1021/jp074728e CCC: $37.00
Published on Web 10/18/2007

$$Cl + CF_3CH_2CH_2OH \rightarrow HCl + \text{products} \quad (1)$$

$$Cl + CF_3CF_2CH_2OH \rightarrow HCl + \text{products} \quad (2)$$

$$Cl + CHF_2CF_2CH_2OH \rightarrow HCl + \text{products} \quad (3)$$

$$Cl + CF_3CHFCF_2CH_2OH \rightarrow HCl + \text{products} \quad (4)$$

Finally, quantum mechanical calculations were performed to determine the bond strengths of C−H and O−H bonds and the ionization potentials of the title compounds to investigate the relationship between structure and reactivity for straight-chain fluorinated alcohols.

2. Experimental Methods

The absolute rate coefficients were measured by using the VLPR-MS apparatus, which has been presented in detail previously.[15] However, a brief description of the apparatus and the experimental procedures followed in the kinetic measurements are presented below.

The reactants enter the Knudsen reactor ($V_{cell} = 107$ cm^3) through separate capillary inlets to suppress back-streaming. The double-wall reactor is thermostated, and its internal surface is coated with a thin Teflon (Du-Pont Teflon 121A) layer to inhibit wall reactions. The reaction mixture escapes from the reactor through a 5 mm orifice into the first stage of a differentially pumped system. A conical skimmer and a tuning fork chopper located in the second vacuum chamber result in the formation of a 200 Hz modulated effusive molecular beam that is collimated into the ionization region of a quadrupole mass spectrometer (Balzers QMG511). The modulated component of the mass spectrometric signal is discriminated and amplified by a lock-in amplifier and subsequently transferred with an A/D card into a microcomputer, where it is stored for subsequent analysis (Figure 1).

Chlorine atoms were produced by flowing a 5% mixture of Cl_2 in helium through a quartz tube, which was enclosed in a 2.45 GHz Evenson microwave cavity operating at 35 W. The quartz tube was coated with a dried slush of a fresh phosphoric acid−boric acid mixture (H_3PO_4/H_3BO_3) to inhibit the recombination of chlorine atoms on the walls. The dissociation of Cl_2 was almost complete, converted into Cl atoms and HCl inside the quartz tube. The absence of any remaining Cl_2 inside the reactor was verified by monitoring the mass peak at m/z 70 in the absence of other reactants. All the kinetic measurements were carried out by setting the ionization electron energy at 19 eV to suppress HCl fragmentation and to avoid its contribution at m/z 35 (<0.3%). The detection limit of Cl atoms in our system was determined to be ca. 1×10^9 molecule cm^{-3}, which is excellent for kinetic experiments.

HFA and Cl_2/He mixture were admitted to the reactor through ca. 150 cm long capillaries with a ca. 0.9 mm internal diameters. Their flow rates (F, molecule s^{-1}) were measured by following the pressure drop in the buffer volumes as a function of time for the actual experimental pressure range. The flow rate of chlorine atoms (F_{Cl}) was derived by assuming a mass balance for all chlorinated species in the discharge tube and the reactor in the absence of any other reactants. The mass balance is given by the expression

$$2\Delta F_{Cl_2} = F_{Cl} + F_{HCl} \quad (I)$$

where $2\Delta F_{Cl_2}$ is the change in F_{Cl_2} with and without the microwave discharge, while F_{Cl} and F_{HCl} are the flow rates of Cl and HCl, respectively. The ratio a_{HCl}/a_{Cl} (see eq III) was also determined by performing accurate titration experiments using the reaction of Cl atoms with n-C_6H_{14} and was found to be 1.3 ± 0.1. Thus the flow rate F_{Cl} was obtained by using eq II

$$F_{Cl} = \frac{2\Delta F_{Cl_2}}{1 + I_{HCl}/(1.3 \times I_{Cl})} \quad (II)$$

The steady-state concentration of all species in the reactor was determined by using the expression

$$[M] = \frac{I_M}{a_{I_M} k_{esc_M} V_R} \quad (III)$$

where I_M is the mass spectral intensity of the selected fragment at 19 eV, V_R is the reactor volume (cm^{-3}), a_{I_M} is the mass calibration factor determined by the linear regression of the intensity of the selected mass spectrometric peaks versus the flow rates $I_M = a_{I_M} F_M$, and k_{esc_M} (eq IV, s^{-1}) is the escape rate coefficient for the species M (s^{-1}), which were measured in separate experiments by following the first-order decays of selected mass peaks after an abrupt halt of their flow (eq V). The escape rate coefficients were determined by using the expressions

$$k_{esc_M} = A_{esc} \sqrt{\frac{T}{M_w}} \quad (IV)$$

$$\ln \frac{I_{Mt}}{I_{M0}} = -k_{esc_M} t \quad (V)$$

where T is the temperature of the reactor, M_w is the molecular weight of the species, and A_{esc} is the escape factor, which for cylindrical reactors depends only on its geometrical characteristics and the diameter of the escape orifice. In our experiments with $A_{esc} = 2.669$ s^{-1} at $T = 303$ K, the residence times for Cl, HCl, $CF_3CH_2CH_2OH$, $CF_3CF_2CH_2OH$, $CHF_2CF_2CH_2OH$, and $CF_3CHFCF_2CH_2OH$ species were 0.127, 0.129, 0.230, 0.264, 0.247, and 0.290 s, respectively.

The fragmentation mass spectra of all the reactants at 19 eV are shown in the Supporting Information. The concentration of each HFA was monitored by selecting its appropriate mass peak that does not have contribution from any possible reaction product. Therefore, several mass peaks were selected and monitored simultaneously for each HFA. In particular, the compounds and the selected peaks were: (i) $CF_3CH_2CH_2OH$, m/z 114, 94, 69, 45, and 31; (ii) $CF_3CF_2CH_2OH$, m/z 100, 83, and 31; (iii) $CHF_2CF_2CH_2OH$, m/z 112, 51, and 31; and (iv) $CF_3CHFCF_2CH_2OH$, m/z 113 and 31. The corresponding concentrations were varied over the ranges of 0.1−7.6, 0.5−48.3, 0.1−7, 0.3−20.3, and 2.9−40.1 in 10^{12} molecule cm^{-3}, respectively.

The a_{Cl} factor was frequently measured in separate calibration experiments (Figure 2) as well as during the kinetic measurements by using a least-squares fit of Cl atom flow rate as a function of the mass spectral intensity at m/z 35. Thus it was verified that the a_{Cl} factors remained constant within 3% during the course of our experiments.

The kinetic measurements were carried out over the temperature range of 273−363 K at very low-pressure conditions (ca. 2 mTorr). The very low-pressure conditions and the small residence times of reactants and products in the reactor exclude the possibility of any secondary bimolecular reactions.[16] The

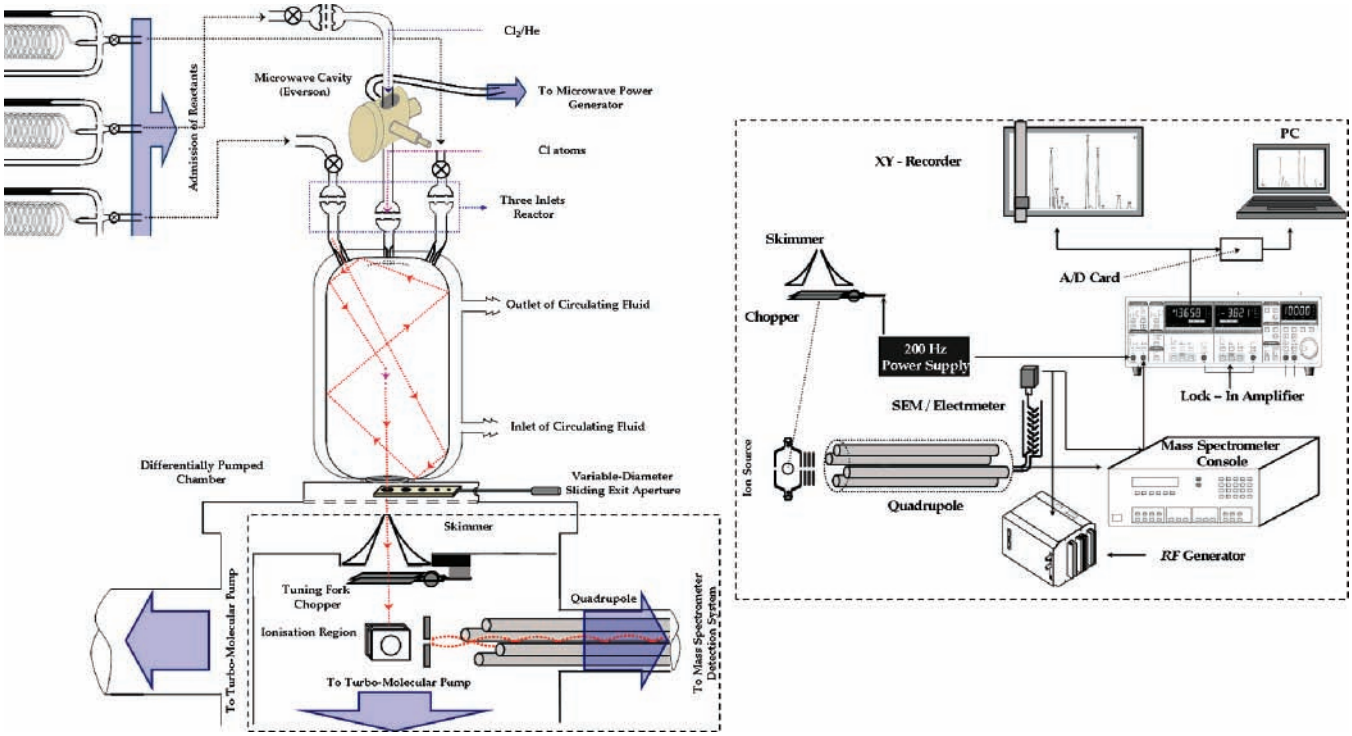

Figure 1. Schematic presentation of the Knudsen reactor and the detection/acquisition system of the VLPR/MS technique.

rate coefficients for all reactions were measured by applying the steady-state equation for both reactants and the stable product HCl. This implies that the total production rate for the species inside the reactor is equal to their loss rate. Therefore, the steady-state equations for Cl atoms, HCl, and HFA are, respectively

$$\Delta[\mathrm{Cl}]k_{\mathrm{esc_{Cl}}} = k_i[\mathrm{HFA}]_r[\mathrm{Cl}]_r;$$

$$\left(\frac{I^0_{\mathrm{Cl}}}{I^{\mathrm{r}}_{\mathrm{Cl}}} - 1\right)k_{\mathrm{esc_{Cl}}} = k_i[\mathrm{HFA}]_{\mathrm{r}} \quad \text{(VI)}$$

$$\Delta[\mathrm{HFA}]k_{\mathrm{esc_{HFA}}} = k_i[\mathrm{Cl}]_{\mathrm{r}}[\mathrm{HFA}]_{\mathrm{r}};$$

$$\left(\frac{I^0_{\mathrm{HFA}}}{I^{\mathrm{r}}_{\mathrm{HFA}}} - 1\right)k_{\mathrm{esc_{HFA}}} = k_i[\mathrm{Cl}]_{\mathrm{r}} \quad \text{(VII)}$$

$$\Delta[\mathrm{HCl}]k_{\mathrm{esc_{HCl}}} =$$

$$k_i[\mathrm{HFA}]_{\mathrm{r}}[\mathrm{Cl}]_{\mathrm{r}} \quad \frac{\Delta[\mathrm{HCl}]k_{\mathrm{esc_{HCl}}}}{[\mathrm{Cl}]_{\mathrm{r}}} = k_i[\mathrm{HFA}]_{\mathrm{r}} \quad \text{(VIII)}$$

where k_i ($i = 1-4$) are the rate coefficients for reactions 1−4, I^0_{Cl} and I^0_{HFA} are the intensities of Cl atoms and HFA in the absence of the other reactant, and $I^{\mathrm{r}}_{\mathrm{Cl}}$ and $I^{\mathrm{r}}_{\mathrm{HFA}}$ are the intensities in the presence of both reactants. For simplicity, the quantities $(I^0_{\mathrm{Cl}}/I^{\mathrm{r}}_{\mathrm{Cl}} - 1)k_{\mathrm{esc_{Cl}}}$, $(I^0_{\mathrm{HFA}}/I^{\mathrm{r}}_{\mathrm{HFA}} - 1)k_{\mathrm{esc_{HFA}}}$, and $\Delta[\mathrm{HCl}]$-$k_{\mathrm{esc_{HCl}}}/[\mathrm{Cl}]_{\mathrm{r}}$ will be denoted as R_{Cl}, $R_{\mathrm{HFA}i}$, and R_{HCl}, respectively. By comparing the rate coefficients obtained by using the steady-state equation of either reactant, one may obtain information about the mass balance of the reaction and the presence of secondary Cl atoms reactions. HFAs are very unlikely to undergo secondary reactions; thus eq VII is not affected by possible secondary Cl atom reactions. Finally, eq VIII provides additional evidence about the validity of our experimental results, because HCl is the sole reaction product and is in excellent mass balance with both reactants.

2.1. Materials. All reactants were commercially available, and their sources and purities were: Cl_2 (Linde, 99.8%), He (Linde, 99.996%), O_2 (Linde, 99,995%) $CF_3CH_2CH_2OH$ (Aldrich, 98%), $CF_3CF_2CH_2OH$ (Aldrich, 97%), $CHF_2CF_2CH_2OH$ (Aldrich, 98%), and $CF_3CHFCF_2CH_2OH$ (Aldrich, 95%). All HFAs were degassed several times through freeze−pump−thaw cycles at 77 K, and they were analyzed using gas chromatography−mass spectrometry (GC-MS) after subjecting the samples to fractional distillation. The results of the gas chromatography analysis as well as their possible effect on kinetic measurements are discussed in the Error Analysis subsection. HFA samples were used undiluted. The mixing ratio of Cl_2 in He was ca. 5%, and the mixtures were prepared by condensing Cl_2 at liquid nitrogen temperature, degassing several times, and pressurizing the storage bulb with the appropriate pressure of He. The mixing ratio of the prepared mixture was also calibrated by flow-calibration experiments using a flow of neat Cl_2 as a reference. The results of the two different titrating techniques were in excellent agreement within 1%.

3. Results and Discussion

The rate coefficients were obtained by least-squares fits of the R_{Cl} versus [HFA] data to eq VI at different temperatures. HFA concentrations were measured by employing eq III. A typical rate determination plot at $T = 303$ K for $CF_3CH_2CH_2$-OH is presented in Figure 3. The precision of all measurements was always better than 3%. In addition, the rate coefficients k_i ($i = 1-4$) were also determined by using the steady-state eqs VII and VIII for HFA and HCl molecules, respectively. A summary of the experimental conditions and the rate coefficients measured in each experiment as well as the final $k_i(T)$ after combining the experiments at each temperature and fitting the data using the least-squares method are given in Tables 1 and 2, respectively. The quoted uncertainties in Tables 1 and 2 represent the 2σ precision of the least-squares fits.

3.1. Kinetic and Mechanistic Investigation. Mass spectrometric analysis of the reaction mixtures in title reactions

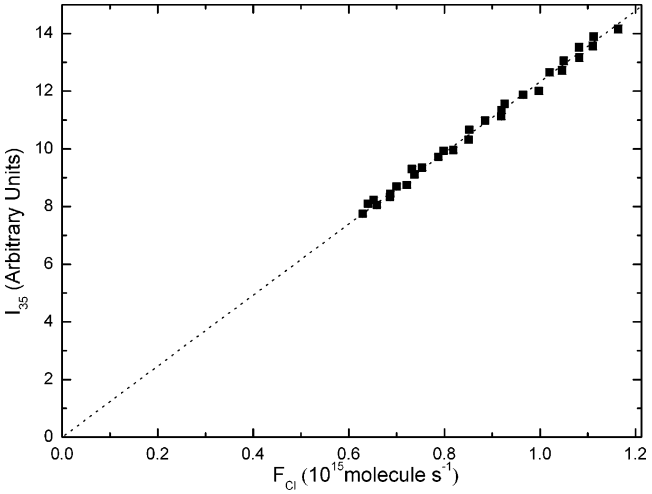

Figure 2. Typical plot for the measurement of the calibration factor of Cl atoms (a_{Cl}). a_{Cl} is determined by the least-squares fit of the parent mass spectral intensity of Cl atoms as a function of the flow rate of Cl atoms inside the reactor.

confirmed HCl at *m*/*z* 36 to be the primary reaction product. Thus, all four reactions proceed via a hydrogen metathesis mechanism, and the possible reaction pathways are

$$Cl + CF_3CH_2CH_2OH \xrightarrow{k_1} \begin{cases} HCl + CF_3CH_2CHOH & (1a) \\ HCl + CF_3CHCH_2OH & (1b) \\ HCl + CF_3CH_2CH_2O & (1c) \end{cases}$$

$$Cl + CF_3CF_2CH_2OH \xrightarrow{k_2} \begin{cases} HCl + CF_3CF_2CHOH & (2a) \\ HCl + CF_3CF_2CH_2O & (2b) \end{cases}$$

$$Cl + HCF_2CF_2CH_2OH \xrightarrow{k_3} \begin{cases} HCl + HCF_2CF_2CHOH & (3a) \\ HCl + CF_2CF_2CH_2OH & (3b) \\ HCl + HCF_2CF_2CH_2O & (3c) \end{cases}$$

$$Cl + CF_3CHFCF_2CH_2OH \xrightarrow{k_4} \begin{cases} HCl + CF_3CHFCF_2CHOH & (4a) \\ HCl + CF_3CFCF_2CH_2OH & (4b) \\ HCl + CF_3CHFCF_2CH_2O & (4c) \end{cases}$$

The least-squares fit of the plot of R_{Cl} versus $[CF_3CH_2CH_2OH]_r$ produced identical rate coefficients by measuring the $CF_3CH_2CH_2OH$ concentration based on either mass fragments *m*/*z* 114 (M^+), 94 ($M - HF^+$), 45 ($M - CF_3^+$), or 31 ($M - CF_3CH_2^+$, 100%). In particular, the parent peak at *m*/*z* 114 and the fragment peak at *m*/*z* 45 cannot have any contribution from primary radical products. For comparison purposes, the above four mass peaks were simultaneously monitored. The present rate coefficients were determined by using the highest mass peak at *m*/*z* 31. However, by using the mass peak at *m*/*z* 69 ($M - CH_2CH_2OH^+$) the rate coefficients were systematically lower due to the contribution to this peak by the primary radical product. Moreover, application of the steady-state equation for $CF_3CH_2CH_2OH$ led to identical rate coefficient values within experimental error, which verifies the absence of any secondary Cl atom reactions.

The rate coefficient for reaction 2 was obtained by monitoring $CF_3CF_2CH_2OH$ using either mass peak at *m*/*z* 100 ($M - CF_2^+$), 83 ($M - CF_2OH^+$), or 31 ($M - CF_3CF_2^+$, 100%), which all yielded identical rate coefficient values. However, the present analysis was based on the highest mass peak at *m*/*z* 31, which is also free from any radical product contribution.

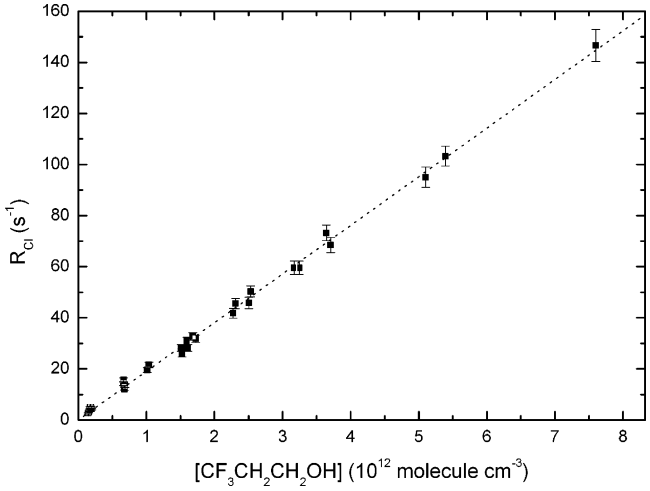

Figure 3. Typical plot for the determination of the rate coefficient for the reaction of Cl atoms with $CF_3CH_2CH_2OH$, at $T = 303$ K, based on the steady state for Cl atoms. The error bars include both precision and accuracy of the measurement.

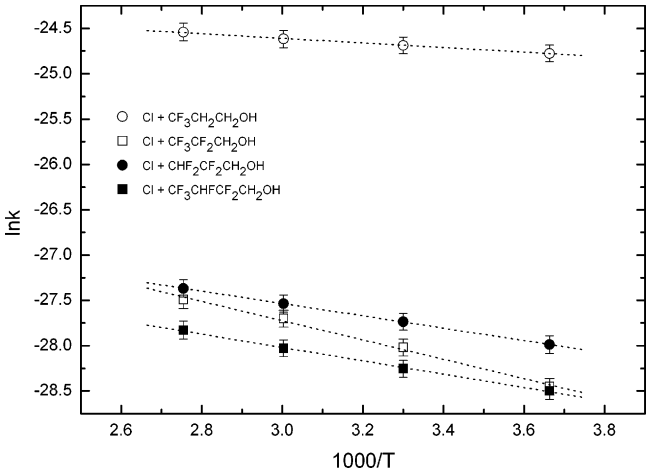

Figure 4. Arrhenius plots for the reactions of Cl atoms with the title HFAs in the temperature range of $T = 273-363$ K. The error bars include both random and systematic uncertainties at a 95% level of confidence (2σ).

The rate coefficient for reaction 3 was obtained by monitoring $CHF_2CF_2CH_2OH$ using either mass peak at *m*/*z* 112 ($M - HF^+$) or 31 ($M - CHF_2CF_2^+$, 100%). However, the use of the *m*/*z* 51 peak ($M - CF_2CH_2OH^+$) yielded lower rate coefficients, which is a clear indication that the primary radical product contains the $-CHF_2$ group. In addition, the presence of pathway 3b should result in a systematic increase of the peak at *m*/*z* 31 (CH_2OH^+) and thus to an underestimation of the rate coefficient. However, the rate coefficient values obtained by using mass peaks at *m*/*z* 112 and 31 were identical, which suggests that the radical product does not contain the CH_2OH group. Furthermore, the high O−H bond strength excludes the presence of pathway 3c, suggesting that reaction 3 occurs primarily by pathway 3a.

Finally, the rate coefficient for reaction 4 was obtained by monitoring $CF_3CHFCF_2CH_2OH$ using either mass peaks at *m*/*z* 113 ($M - CF_3^+$) or 31 ($M - CF_3CHFCF_2^+$, 100%), which gave identical rate coefficient values. The $M - CF_3^+$ fragment does not have any contribution from radical products. However, the kinetic measurements were mainly performed by using the highest peak at *m*/*z* 31.

TABLE 1: Typical Experimental Data[a]

T (K)	[Cl]	R_{Cl}	[HFA]	k
		$CF_3CH_2CH_2OH$		
273	0.14−0.91	3.7−62.0	0.11−3.99	17.4 ± 0.4
273	0.14−0.86	4.46−67.7	0.16−3.44	17.4 ± 0.5
303	0.06−0.84	3.9−164.0	0.17−7.75	19.0 ± 0.5
303	0.10−0.88	2.63−73.2	0.16−4.03	18.5 ± 0.3
303	0.19−0.82	4.16−42.67	0.22−2.92	18.3 ± 0.6
303	0.12−0.62	2.31−47.39	0.14−2.63	19.1 ± 0.7
333	0.16−0.71	2.46−41.42	0.08−1.97	20.7 ± 0.4
333	0.16−0.77	3.76−65.28	0.15−3.48	19.6 ± 0.6
333	0.14−0.72	4.58−77.35	0.14−3.65	21.0 ± 0.5
363	0.10−3.56	5.25−49.21	0.37−1.97	21.8 ± 0.7
363	0.13−0.32	3.05−21.2	0.10−0.87	22.2 ± 0.8
363	0.19−0.37	3.48−19.86	0.32−1.58	22.3 ± 0.7
		$CF_3CF_2CH_2OH$		
273	0.44−1.11	0.24−12.48	1.89−28.27	0.42 ± 0.02
273	0.34−0.96	0.40−15.04	0.74−30.18	0.45 ± 0.03
303	0.15−0.55	0.46−22.84	0.38−29.26	0.70 ± 0.01
303	0.21−1.64	1.15−22.27	2.00−34.04	0.68 ± 0.01
303	0.15−1.05	1.24−30.57	0.37−41.27	0.66 ± 0.02
303	0.35−1.72	0.19−20.34	0.43−3.35	0.71 ± 0.03
333	0.20−1.19	1.12−33.78	0.50−35.17	0.93 ± 0.02
333	0.08−0.76	3.87−39.71	0.85−44.12	0.95 ± 0.02
333	0.07−0.77	0.78−45.53	0.80−46.10	0.94 ± 0.03
333	0.36−1.20	0.83−28.72	0.60−30.52	0.94 ± 0.02
363	0.07−0.51	0.64−60.92	0.50−48.29	1.14 ± 0.03
363	0.05−0.32	2.05−36.55	0.70−24.02	1.13 ± 0.03
363	0.11−0.50	0.58−35.96	0.78−40.79	1.18 ± 0.05
363	0.19−0.66	0.71−30.82	0.57−33.57	1.16 ± 0.03
		$CHF_2CF_2CH_2OH$		
273	0.39−0.68	0.30−8.68	0.40−15.12	0.66 ± 0.02
273	0.66−1.72	1.40−14.98	1.33−18.74	0.70 ± 0.01
273	0.59−0.99	1.36−7.78	1.32−12.92	0.68 ± 0.02
273	0.28−0.79	0.65−9.48	0.50−16.84	0.73 ± 0.03
303	0.25−1.33	1.05−15.49	0.76−13.85	0.93 ± 0.03
303	0.23−12.74	0.40−14.23	0.37−18.08	0.91 ± 0.02
303	0.32−0.99	0.85−24.23	0.12−20.33	0.90 ± 0.01
303	0.76−1.29	0.90−8.11	0.58−7.48	0.95 ± 0.01
333	0.49−1.08	2.33−16.58	1.50−15.48	1.10 ± 0.02
333	0.50−0.97	1.19−9.90	0.65−9.57	1.09 ± 0.04
363	0.23−0.45	1.91−12.24	0.51−10.09	1.27 ± 0.03
363	0.24−0.56	0.91−15.16	0.87−14.82	1.25 ± 0.02
363	0.34−0.88	0.68−17.70	0.37−13.68	1.32 ± 0.04
		$CF_3CHFCF_2CH_2OH$		
273	0.73−1.53	1.65−12.38	3.28−29.23	4.21 ± 0.14
273	0.69−1.71	1.15−14.71	3.49−33.49	4.22 ± 0.10
273	0.74−2.37	0.71−15.10	2.63−36.55	4.16 ± 0.12
303	0.42−1.28	1.48−21.52	3.70−40.11	5.29 ± 0.15
303	0.75−1.49	1.19−10.52	2.93−20.83	5.41 ± 0.10
303	0.54−13.33	3.88−18.05	5.82−32.88	5.39 ± 0.08
333	0.60−1.32	2.36−16.02	2.93−22.49	6.80 ± 0.11
333	0.48−1.12	1.92−18.97	3.39−27.39	6.63 ± 0.16
363	0.17−0.53	1.30−26.27	2.09−25.90	8.01 ± 0.25
363	0.30−0.58	5.69−22.191	10.75−28.76	7.92 ± 0.36
363	0.42−10.28	1.63−18.02	2.02−22.31	8.30 ± 0.30

[a] Steady-state concentrations of Cl atoms and HFA are expressed in 10^{12} molecule cm^{-3}. $R_{Cl} = ([Cl]_0/[Cl]_r - 1)k_{esc_{Cl}} = (I_{Cl_0}/I_{Cl_r} - 1)k_{esc_{Cl}}$ (s^{-1}), where the subscript 0 denotes the steady-state concentration in the absence of HFA. The quoted uncertainties in rate coefficients (k in 10^{-12} cm^3 molecule^{-1} s^{-1}) represent the 2σ precision of the least-squares fits.

In general, for all four reactions, the absence of contributions to the peak at m/z 31 suggests that the radical products do not contain the $-CH_2OH$ group; therefore the abstraction of a methylenic hydrogen adjacent to the $-OH$ group is the most likely reaction pathway.[11,13,14]

3.2. Temperature Dependence. The kinetic experiments were performed at four different temperatures: 273, 303, 333, and 363 K. The temperature dependence of the rate coefficients was determined by the least-squares fits of the plot of ln k_i versus $1/T$ (Figure 4). The k_i values are summarized in Table 2 and were obtained by the least-squares fit of the plots of R_{Cl} versus [HFA] at each temperature. The quoted 2σ uncertainties take into account both random and systematic errors. The Arrhenius expressions obtained for all four reactions are given below

TABLE 2: Rate Coefficients (cm^3 molecule^{-1} s^{-1}) at the Temperatures 273, 303, 333, and 363 K[a]

	T (K)			
	273	303	333	363
	$CF_3CH_2CH_2OH$			
$k/10^{-11}$ (RCl)	1.74 ± 0.04	1.90 ± 0.03	2.04 ± 0.07	2.20 ± 0.08
$k/10^{-11}$ (RHCl)	1.68 ± 0.15	1.85 ± 0.10	2.13 ± 0.10	2.31 ± 0.15
$k/10^{-11}$ (RHFA)	1.69 ± 0.09	1.97 ± 0.07	2.07 ± 0.12	2.12 ± 0.09
$[Cl]/10^{11}$	1.37−9.06	0.56−8.81	1.37−8.44	0.39−5.37
$[HFA]/10^{12}$	0.12−4.35	0.14−7.58	0.06−2.88	0.08−5.18
no. of points	24	60	36	35
	$CF_3CF_2CH_2OH$			
$k/10^{-13}$ (RCl)	4.40 ± 0.09	6.78 ± 0.14	9.32 ± 0.28	11.50 ± 0.45
$k/10^{-13}$ (RHCl)	4.22 ± 0.09	6.86 ± 0.23	8.92 ± 0.51	11.59 ± 0.60
$k/10^{-13}$ (RHFA)	4.34 ± 0.09	6.68 ± 0.20	9.22 ± 0.42	11.35 ± 0.63
$[Cl]/10^{11}$	3.42−11.15	1.51−17.17	0.75−12.00	0.55−6.64
$[HFA]/10^{12}$	0.74−30.18	0.34−41.27	0.50−46.10	0.50−48.29
no. of points	30	56	59	59
	$CHF_2CF_2CH_2OH$			
$k/10^{-13}$ (RCl)	7.00 ± 0.25	9.00 ± 0.09	11.00 ± 0.30	13.00 ± 0.40
$k/10^{-13}$ (RHCl)	7.16 ± 0.34	9.18 ± 0.40	10.6 ± 0.50	13.21 ± 0.63
$k/10^{-13}$ (RHFA)	6.84 ± 0.29	8.92 ± 0.34	11.2 ± 0.45	12.73 ± 0.69
$[Cl]/10^{11}$	2.82−18.74	2.33−13.28	4.90−10.83	2.27−8.85
$[HFA]/10^{12}$	0.40−18.74	0.27−20.33	0.65−15.48	0.37−14.82
no. of points	43	43	28	28
	$CF_3CHFCF_2CH_2OH$			
$k/10^{-13}$ (RCl)	4.20 ± 0.12	5.36 ± 0.10	6.72 ± 0.15	8.20 ± 0.36
$k/10^{-13}$ (RHCl)	4.18 ± 0.12	5.63 ± 0.14	6.44 ± 0.30	8.68 ± 0.35
$k/10^{-13}$ (RHFA)	4.22 ± 0.29	5.42 ± 0.34	6.90 ± 0.45	8.33 ± 0.69
$[Cl]/10^{11}$	6.93−23.75	4.15−14.92	5.80−13.65	1.73−10.28
$[HFA]/10^{12}$	2.63−36.55	2.93−40.11	2.93−27.39	2.02−28.76
no. of points	38	41	25	29

[a] The species to which the steady-state approximation was applied for measuring the rate coefficient is denoted in parentheses. The quoted uncertainties represent the 2σ precision of the measurements.

$$k_1 = (4.42 \pm 0.48) \times 10^{-11} \exp(-255 \pm 20/T)$$

$$k_2 = (2.23 \pm 0.31) \times 10^{-11} \exp(-1065 \pm 106/T)$$

$$k_3 = (8.51 \pm 0.62) \times 10^{-12} \exp(-681 \pm 72/T)$$

$$k_4 = (6.18 \pm 0.84) \times 10^{-12} \exp(-736 \pm 42/T)$$

The uncertainties in the exponential part of the Arrhenius expressions reflect the 2σ precision of the least-squares fits, while the uncertainties in pre-exponential factors were estimated by the expression $dA = A \times d \ln A$, taking also into account the systematic errors of the measurements.

The uncertainties of our measurements are also expressed in terms of the NASA/JPL recommendation[17] using eq IX

$$f(T) = f(303\ \text{K}) \exp\left(\left|g\left(\frac{1}{T} - \frac{1}{303}\right)\right|\right) \qquad \text{(IX)}$$

For reactions 1−4 the estimated g_i values are $g_1 = 40$, $g_2 = 35$, $g_3 = 40$, and $g_4 = 45$, while for all four reactions the uncertainty of our measurements at $T = 303$ K was considered to be 11%; therefore $f(303\ \text{K}) = 1.11$.

A comparison with the available data in the literature is presented in Table 3. The quoted uncertainties represent the 2σ

TABLE 3: Kinetic Parameters and Rate Coefficients at $T = 303$ K for the Reactions of Cl Atoms with the Partially Fluorinated Alcohols of the Present Study and Comparison with Available Literature Data at $T = 298$ K[a]

reaction	k_{Cl}	A	E_a/R	technique/reference
$Cl + CF_3CH_2CH_2OH$	19.0 ± 1.7	4.42 ± 0.48	255 ± 20	this work
	22.4 ± 4.0			RR−GC−FID/FTIR[11]
	15.9 ± 2.0			RR−FTIR[12]
$Cl + CF_3CF_2CH_2OH$	0.68 ± 0.07	2.23 ± 0.31	1065 ± 106	this work
	0.65 ± 0.05			RR/FTIR[13]
$Cl + HCF_2\ CF_2CH_2OH$	0.90 ± 0.08	0.85 ± 0.06	681 ± 72	this work
$Cl + CF_3CHFCF_2CH_2OH$	0.54 ± 0.05	0.62 ± 0.08	736 ± 42	this work

[a] Rate coefficients are in 10^{-12} cm^3 molecule^{-1} s^{-1}, pre-exponential Arrhenius factors are in 10^{-11} cm^3 molecule^{-1} s^{-1}, and E_a/R are in K. The quoted uncertainties represent the 2σ and include both systematic and random errors (RR-GC-FID/FTIR, relative rate gas chromatography flame ionization detector/Fourier transform infrared; RR-FTIR, relative rate/Fourier transform infrared).

TABLE 4: Ion Fragments Detected after Oxidation of the Primary Dehydrogenated Radicals

	oxidation products		
parent alcohol	aldehydes	m/z (M^+)	m/z detected
$CF_3CH_2CH_2OH$	$CF_3CH_2CH_2C(O)H$	112	112 (M^+)
$CF_3CF_2CH_2OH$	$CF_3CF_2C(O)H$	148	79 ($M - CF_3^+$)
$CHF_2CF_2CH_2OH$	$CHF_2CF_2C(O)H$	130	79 ($M - CHF_2^+$)
$CF_3CHFCF_2CH_2OH$	$CF_3CHFCF_2C(O)H$	180	111 ($M - CF_3^+$)

precision of the fits. To our knowledge, the present study is the first temperature-dependent absolute rate coefficient measurement for reactions 1−4. Reaction 1 has been studied by Kelly et al.[11] and Hurley et al.[12] at room-temperature conditions using relative rate techniques, and our result is in reasonably good agreement with both studies. The deviation of 30% between the two available relative rate studies might be due to the different reference reactions that they used, which is discussed extensively by Hurley et al. As far as reaction 2 is concerned, there is only one study in the literature by Hurley et al.[13] at 296 K. The measured rate coefficients at room temperature from both studies are in excellent agreement within experimental uncertainties. For reactions 3 and 4, there are no available data in the literature to be compared with our measured values.

3.3. Analysis of Oxidation End Products. For the oxidation experiments, a three-inlet reactor was used to allow the separate admission of molecular O_2 to the reaction mixture. The volume of the reactor was 290 cm^3, and the escape aperture was set to 2 mm to increase the residence time of reactants and to enhance the presence of secondary reactions. These experiments were conducted by using high HFA concentrations to ensure high radical yields and an excess of O_2 molecules (ca. 10^{15} molecule cm^{-3}). The end reaction products were analyzed by mass spectrometry. The electron voltage in the ionization region was varied between 70 and 19 eV to counterbalance sensitivity versus fragmentation and obtain the optimum conditions for the final oxidation product detection.

In all four cases, fluorinated aldehydes were detected as the primary final oxidation products (Table 4). In particular, CF_3CH_2CHO was verified by the appearance of a new mass peak at m/z 112 (M^+) and the increase of m/z 29 ($M - CF_3CH_2^+$). The absence of any other products indicates that the primary reactions proceed mainly via the abstraction of the α-methylenic hydrogen. The results for all four reactions were consistent with this mechanism, and the fragments detected, apart from that at m/z 29 ($M - R_F^+$) which was present in all cases, are summarized in Table 4. Thus, the overall Cl-atom-initiated oxidation mechanism for the title HFAs may be given by the following reaction scheme

$$R_F{-}CH_2OH + Cl \rightarrow R_F{-}CHOH + HCl \qquad (5)$$

$$R_F{-}CHOH + O_2 \rightarrow R_F{-}C(O)H + HO_2 \qquad (6)$$

where $R_F = -CH_2CF_3$, $-CF_2CF_3$, $-CF_2CHF_2$, and $-CH_2CHFCF_3$.

3.4. Error Analysis. The precision of the kinetic measurements was always better than 3% including both repeatability and reproducibility at a 95% level of confidence (2σ). Moreover, the uncertainties in the measured mass spectral intensities under steady-state conditions, the temperatures employed, and the volume of the reactor were less than 1%. The major error in the concentration of HFA is attributed to the flow rates measured and is reflected in the mass spectrometric calibration factor a_M of a species M. Taking into account the precision in measuring pressures during flow-calibration experiments, the uncertainty in a_M was determined to be ca. 3%. Furthermore, the uncertainty of the escape rate coefficients of the species M (k_{esc_M}) is ca. 2%. Thus, we estimate that the 2σ systematic uncertainties in our experiments are ca. 9%.

Other sources of uncertainties may stem from secondary reactions of Cl atoms with wall surfaces or minor sample impurities. All four samples were subjected to GC-MS analysis, revealing that the purity was always higher than 99.5%, and no impurity was quantified at levels higher than 0.2%. We were not able to identify the nature of these minor impurities and consequently to know their relative reactivity toward Cl atoms. Therefore, we performed separate experiments by using the steady-state equation for HFA (eq VII), a scheme that is independent of minor sample impurities or any secondary Cl atoms reactions. The rate coefficients obtained were in very good agreement (within 5%) of those obtained by using the steady-state equation for Cl atoms (eq VI), indicating that HFA samples were sufficiently pure and any interference of secondary chemistry was negligible. In addition, there was a very good agreement among the kinetic results obtained by using the steady-state equations of HFA, Cl atoms, or HCl, indicating the absence of wall reactions.

3.5. Theoretical Calculations of the C−H Bond Strengths and the Ionization Potentials of Partially Fluorinated Alcohols. All calculations were performed with the Gaussian 98 program suite[18] by using three density functional theory functionals in combination with a variety of basis sets. The B3P86 functional[19,20] was employed in all geometry optimizations, vibrational frequency calculations, and the calculation of the C−H and O−H bond strengths. The B3P86 functional has been shown to yield reliable bond strengths of closed-shell species with an average deviation from experimental values on the order of 5 kJ mol^{-1}.[21,22] The calculation of ionization potentials was performed by the B3LYP and B3PW91 functionals,[19,20,23,24] which have been shown to be sufficiently reliable for the calculation of molecular ionic properties.[22,25] For all closed-shell parent species, the calculations were performed using restricted wavefunctions, while unrestricted wavefunctions were used for the open-shell radical species. To correct for the

deficiencies of the B3P86 electronic structure calculations for open-shell species, the absolute electronic energies of all radicals were increased by the amount of $N_e \times 9 \times 10^{-5}$ hartree, where N_e is the total number of electrons, as has been suggested in a previous study.[21]

Several kinds of basis sets were used to examine the effects of the basis set size and the presence of diffuse functions on the computational accuracy and furthermore to ensure the convergence of the calculated properties to a narrow range of values. Two kinds of basis sets were used: (a) variants of the 6-311G basis set, augmented with d/f polarization functions and diffuse functions, denoted by 6-311++G(2d,p) and 6-311++G(3df,2p)[26−28] and (b) correlation-consistent basis sets, of double and triple-ζ quality, namely, aug-cc-pVDZ, cc-pVTZ, and aug-cc-pVTZ,[29,30] where the prefix aug stands for the diffuse function augmented variants.

The geometry optimizations and vibrational frequency calculations were carried out at the B3P86/aug-cc-pVDZ level of theory for all species. Several conformations were selected for the parent molecules and their singly dehydrogenated radicals as the initial structures prior to the geometry optimization to locate all possible local minima on the potential energy surfaces. For all stationary points, the absence of imaginary vibrational frequencies indicated that they correspond to true minima at the B3P86/aug-cc-pVDZ potential energy surface. The electronic energies of all local minima were further refined by single-point calculations using a larger basis set at the B3P86/aug-cc-pVTZ level of theory, and those with the lowest energies were chosen to represent the global potential energy minima. However, the energy differences between the various minima for all species were always lower than 10 kJ mol^{-1} with the exception of a 15 kJ mol^{-1} difference for the $CF_3CHFCF_2CH_2O$ radical conformers. The optimized structural parameters of all species and their harmonic vibrational frequencies are shown in the Supporting Information (Tables 1 and 2, respectively).

Absolute electronic energies for all species at higher levels of theory comprising the B3P86, B3LYP, and B3PW91 functionals with larger basis sets were obtained by single-point calculations using the optimized geometries. The zero-point and the thermal energies at 298.15 K were derived by considering the rigid-rotor and the harmonic oscillator approximations after scaling all vibrational frequencies by 0.9723.[21] These enthalpic corrections were subsequently added to the absolute electronic energies to yield the absolute enthalpies for each species and, finally, the C−H and O−H bond strengths. The ionization potentials (IPs) were calculated as the difference between the sum of absolute energies for the parent alcohol and its singly ionized radical cation.

The absolute electronic energies for all species were found to depend on the arrangement of the −OH group, as noted previously.[14] For CH_3CH_2OH and CH_3CHOH, there is a slight increase of the energy by ca. 1 kJ mol^{-1} when the −OH group is arranged toward the $-CH_3$ group due to the unfavorable steric repulsions. However, for all HFAs and their hydroxy radicals, there is an energy decrease when the −OH group is facing the F atoms due to the attractive intramolecular C−F···H−O interactions. The energy barrier of the OH internal rotation depends on the degree of substitution by fluorine atoms, reaching a maximum of ca. 12 kJ mol^{-1} for $CF_3CF_2CH_2OH$. In the case of the radicals R_F−CHOH, the rotation of the OH group around the C−O bond is accompanied by even greater energy changes due to the stabilizing effect of a π-type orbital overlap in the C−O bond. This overlap is maximized when all atoms in the −CHOH moiety lie on the same plane, and furthermore the two hydrogen atoms lie on the same side. When the OH group becomes perpendicular to the C−C−O plane, the electronic energy rises with a maximum of ca. 30 kJ mol^{-1} for the CF_3-CF_2CHOH radical. In addition, the intermolecular C−F···H−O interactions are even stronger in these hydroxyl radicals, and an energy increase of 13.5 kJ mol^{-1} is calculated when the hydroxylic hydrogen faces in the opposite direction of the $-CF_2-$ group for the CF_3CF_2CHOH radical.

All C−H and O−H bond strengths for the title alcohols and the corresponding nonfluorinated ones as well as for several fluorinated C1 and C2 alkanes and alcohols were calculated at five levels of theory, all comprising of the B3P86 functional in combination with the basis sets aug-cc-pVDZ, cc-pVTZ, aug-cc-pVTZ, 6-311++G(2df,p), and 6-311++G(3df,2p). The average deviation of the calculated from experimentally known values (inferred from the experimental enthalpies of formation[17,31]) was improved from ca. 4 to 2 kJ mol^{-1} by the empirical adjustment of the UB3P86 energies.[21] Furthermore, the variation of calculated bond strengths at those levels of theory was small and never exceeded 4 kJ mol^{-1}, which suggests that sufficient convergence to a narrow range of values has been achieved. However, a negligible dependence on the size of the basis set was noted, and the accuracy of the calculated bond strengths was slightly improved by the presence of diffuse functions. The average values of the empirically corrected results at the three most accurate levels of theory (B3P86/aug-cc-pVTZ, B3P86/aug-cc-pVDZ, and B3P86/6-311++G(2df,p)) are shown in the Supporting Information. The largest deviation from experimental values (10 kJ mol^{-1}) was presented by the H−CH_2CH_2OH bond, and all remaining deviations were lower than 6 kJ mol^{-1}. Therefore, the uncertainty of the reported bond strengths of C−H and O−H bonds in fluorinated alcohols is estimated to be $\pm$10 kJ mol^{-1}.

As shown in the Supporting Information, the C−H bond strengths are lowest for the methylene group next to the oxygen atom, as expected on the basis of the stabilizing effect of the π-electron donation from the oxygen atom to the adjacent carbon-centered radical. The presence of fluorine atoms close to the $-CH_2OH$ moiety tends to strengthen the methylenic C−H bonds due to the electron-attracting effect of F atoms. However, the variation in the bond strengths is relatively small, ranging from 396.0 kJ mol^{-1} for $CH_3CH(-H)OH$ to 411.6 kJ mol^{-1} for $CF_3CHFCF_2CH(-H)OH$. Higher C−H bond strengths are noted for all other groups, ranging from 416.2 kJ mol^{-1} for $CH_3CH(-H)CH_2CH_2OH$ to 442.7 kJ mol^{-1} for $CF_2(-H)CF_2$-CH_2OH. The O−H bonds possess the highest strengths, which are significantly affected by their distance from the fluorine atoms, ranging from 433.7 kJ mol^{-1} for CH_3CH_2O-H to 482.7 kJ mol^{-1} for $CF_3CF_2CH_2O-H$ and finally to 504.8 kJ mol^{-1} for CF_3O-H.

Besides the combined electronic effects of fluorine and oxygen atoms, the presence of intramolecular hydrogen bonds in fluorinated alcohols can also affect the calculated bond strengths. A closer look at the structures of fluorinated alcohols and their carbon-centered radicals reveals that they adopt an arrangement that permits the hydroxylic H atom to approach fluorine atoms (preferably on the β-carbon), thus gaining an extra stabilization by the formation of an intramolecular O−H···F−C hydrogen bond. However, the structural changes accompanying radical formation may alter the H···F distance with a significant effect on the electronic energy of the radical and finally on the C−H bond strength. For example, the H···F distance drops from 2.42 Å in $CF_3CF_2CH_2OH$ to 2.17 Å in CF_3-CF_2CHOH, compared to the smaller relative decrease from 4.40

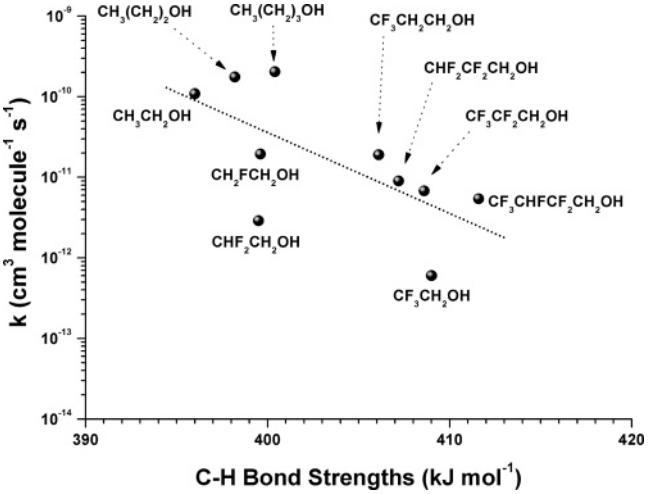

Figure 5. Logarithmic plot of the room-temperature rate coefficients (in cm^3 $molecule^{-1}$ s^{-1}) of chlorine atoms with C2−C4 alcohols vs the strength of their weakest C−H bond (in kJ mol^{-1}).

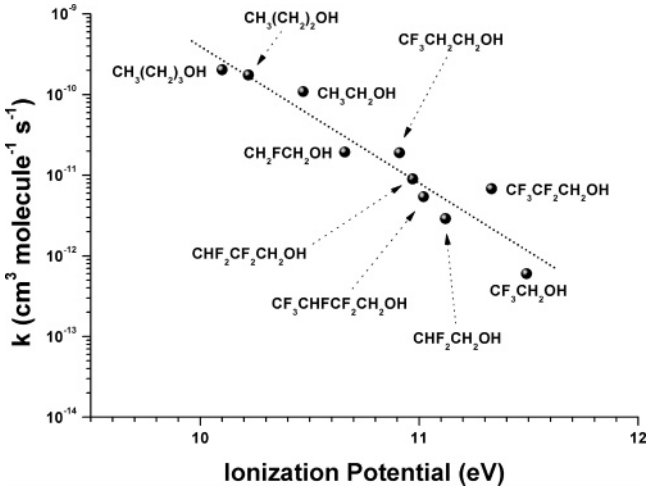

Figure 6. Logarithmic plot of room-temperature rate coefficients (in cm^3 $molecule^{-1}$ s^{-1}) of chlorine atoms with C2−C4 alcohols vs their ionization potential (in eV).

Å in $CF_3CH_2CH_2OH$ to 4.19 Å in CF_3CH_2CHOH. In the latter case, the hydroxylic H atom is too far from the F atoms to gain any substantial stabilization at a distance of this magnitude. Indeed, when the H atom is directed opposite to the $-CF_2-$ group in CF_3CF_2CHOH, the electronic energy rises by 13.5 kJ mol^{-1}, in contrast to a much smaller increase of 2.6 kJ mol^{-1} in CF_3CH_2CHOH. Therefore, the absence of stabilizing intramolecular hydrogen bonds in the fluorinated alkoxy radicals may significantly contribute to the wide range of RO−H (R = alkyl group) bond strengths. For all other radicals and in particular RCHOH, the energetically favorable arrangement of the hydroxyl group toward fluorine atoms compensates for the inductive effects of the latter on bond strengths, because O−H···F distances become shorter and, as a result, stronger.

The ionization potentials of the title alcohols and the corresponding nonfluorinated ones as well as of several simple C1 and C2 fluorinated alkanes and alcohols were calculated at 10 levels of theory, comprising of the B3LYP and B3PW91 functionals and the five basis sets reported above. The mean deviations from experimental values[32] were rather insensitive to the level of theory, on the order of 0.12−0.20 eV. The lowest deviations were presented by the B3PW91 functional, and the agreement with experimental values was slightly deteriorating by the presence of diffuse functions in the basis sets. The average values of the ionization potentials at the three most accurate levels of theory (B3PW91/cc-pVTZ, B3PW91/6-311++G(3df,2p), and B3LYP/cc-pVTZ) are shown in the Supporting Information. By excluding CH_4 and CH_3CH_3, whose calculated values of IPs presented the largest deviations from experiment values (0.7−1.5 eV), the calculated values for the heavier molecules were much closer to experiment, suggesting that the errors in the reported IP values of the present study are on the order of ±0.5 eV. The ionization potentials of the title compounds fall in the narrow range of 10.97−11.33 eV with a weak dependence on the number of fluorine atom substituents.

3.6. Structure−Reactivity Correlations. The quantitative correlation of intrinsic molecular properties with kinetic parameters has been considered as a handy tool for the prediction of rate coefficients, leading to empirical expressions describing structure−reactivity relationships. As appealing to chemical intuition, reaction enthalpy has been commonly employed, sometimes expressed as the linearly dependent strength of the bond broken during the course of a chemical reaction, in the form of the Evans−Polanyi relationship,[33] $E_a = \alpha(-\Delta H_r) + \beta$, where E_a is the activation energy of a reaction, ΔH_r is the reaction enthalpy, and α and β are empirical parameters. It has been recently discussed that reaction barriers are most greatly affected by the ionic states of the molecules involved in a chemical reaction, and as a result, ionization potentials and electronic affinities should be better employed for structure−reactivity correlations.[34,35] However, for hydrogen metathesis reactions of an electrophilic radical (Cl or OH) with a series of molecules possessing similar structural characteristics, these two types of correlation are expected to converge, because trends in the lowest C−H bond strengths and the corresponding ionization potentials are generally similar.[32] Furthermore, examination of all C−H bond strengths in a molecule may indicate the most probable sites of the initial hydrogen atom abstraction and, consequently, the final atmospheric oxidation products.

The correlation of all available room-temperature rate coefficients of chlorine atoms with C2−C4 alcohols versus the strength of their weakest C−H bond and their ionization potential was attempted. Wherever possible, the experimentally available values of the molecular properties were employed; the values derived theoretically in the present study were employed in all other cases. The logarithmic plot of the rate coefficients versus the C−H bond strengths is shown in Figure 5. A linear least-squares fit of the data yields the expression $\log(k)$ (in cm^3 $molecule^{-1}$ s^{-1}) = (29.7 ± 15.9) − (0.10 ± 0.04) × (C−H bond strength (kJ mol^{-1})). The deviations from the fit are rather large, and the rate coefficients for CHF_2CH_2OH and CF_3CH_2OH deviate almost by an order of magnitude. As discussed by Kelly et al.,[11] the divergence in the measured rate coefficients between alcohols and hydrocarbons in general, possessing a different positioning and degree of fluorination, cannot be interpreted considering only the inductive effects of F atoms and the subsequent strengthening of the C−H bonds. For instance, although the $CF_3CHFCF_2CH(-H)OH$ and $CF_3CH_2CH(-H)OH$ bond strengths differ by ca. 5 kJ mol^{-1}, their rate coefficients differ by a factor of ca. 35. It is more likely that the electronic and steric effects of F substituents affect directly the transition state with a subsequent effect on, among others, the activation entropy of the system, $\Delta S^{\ddagger}$, which is entirely neglected in correlations employing bond strengths. Positioning and degree of fluorination can potentially have both synergetic as well as contradictory roles in the stabilization of the transition state, resulting in a complicated effective function for the prediction of rate coefficients. The last statement can

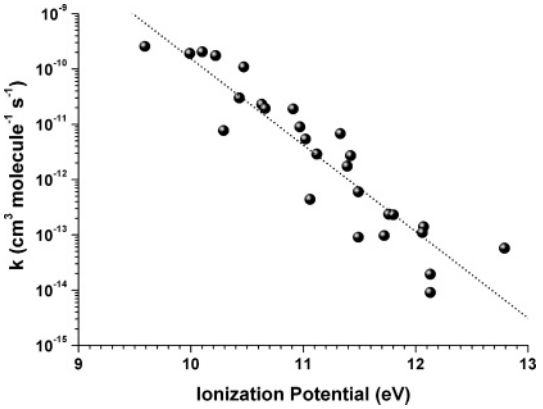

Figure 7. Logarithmic plot of room-temperature rate coefficients (in cm^3 $molecule^{-1}$ s^{-1}) of chlorine atoms with C2−C4 alcohols and C2−C5 ethers vs their ionization potential (in eV).

TABLE 5: Room-Temperature Rate Coefficients for Several Hydrofluorocarbons and Fluorinated Alcohols with OH Radicals and Cl Atoms (in 10^{-15} cm^3 $molecule^{-1}$ s^{-1}) and the Corresponding Tropospheric Lifetimes τ (in years)

	k_{OH}[a]	k_{Cl}[a]	τ_{OH}[b]	τ_{Cl}[b]	τ_{eff}[b]
CH_2F_2	10	50	3.2	63	3.0
CHF_3	0.3	0.003	106	1.1×10^6	105
CHF_2CH_3	35	260	0.9	12	0.8
CF_3CH_3	1.2	0.03	26	1.1×10^5	26
CF_3CH_2F	4.2	1.5	7.5	2112	7.5
CF_3CHF_2	1.9	0.2	17	1.6×10^4	17
$CF_3CH_2CHF_2$	7.0	6.9[c]	4.5	459	4.5
$CF_3CH_2CF_3$	0.3	0.01[d]	106	3.2×10^5	106
CF_3CHFCF_3	1.7	0.04[e]	19	7.9×10^4	19
$CF_3CH_2CF_2CH_3$	5.7	1.1[d]	5.6	2880	5.5
$CF_3CHFCHFCF_2CF_3$	3.4		9.3		9.3
CH_2FCH_2OH	1710[f]	19 400[g]	0.02	0.16	0.02
CHF_2CH_2OH	252[h]	2900[g]	0.13	1.09	0.11
CF_3CH_2OH	103[i]	600[g]	0.31	5.3	0.29
$CF_3CH_2CH_2OH$		19000[j]		0.17	
$CF_3CF_2CH_2OH$	104[k]	6800[j]	0.31	0.47	0.18
$CHF_2CF_2CH_2OH$		9000[j]		0.35	
$CF_3CHFCF_2CH_2OH$	130[l]	5400[j]	0.24	0.59	0.17

[a] Rate coefficients for the reactions of most hydrofluorocarbons with OH and Cl are taken from ref 17. [b] τ_{OH} and τ_{Cl} are based on diurnal average concentrations [OH] and [Cl] of 1×10^6 [36] and 1×10^4 molecule cm^{-3},[37] respectively, and τ_{eff} represents the effective lifetime, according to the expression $1/\tau_{eff} = 1/\tau_{OH} + 1/\tau_{Cl}$. [c] Reference 41. [d] Reference 42. [e] Reference 43. [f] Reference 44. [g] Reference 14. [h] Reference 45. [i] Reference 46. [j] This work. [k] Reference 13. [l] Reference 47.

interpret to some extent the failure of bond strengths, which depend only on the end points of the reaction scheme, to provide an accurate estimation of reaction rates. The logarithmic plot of the room-temperature rate coefficients versus the ionization potentials is shown in Figure 6. A linear least-squares fit yields the expression $\log(k)$ (in cm^3 $molecule^{-1}$ s^{-1}) = (7.6 ± 2.1) − (1.70 ± 0.19) × (ionization potential (eV)). The correlation is better than that of bond strengths, suggesting that ionization potentials represent a better reactivity index for these compounds. A collective plot for 27 molecules, comprising 10 C2−C4 alcohols and 17 C2−C5 ethers (taken from a recent work[22]) is shown in Figure 7. The correlation remains good with an average deviation by a factor 2 in the rate coefficients, providing a rough estimation method of the rate coefficients for oxygen-containing CFC alternatives. A linear least-squares fit yields the expression $\log(k)$ (in cm^3 $molecule^{-1}$ s^{-1}) = (5.8 ± 1.4) − (1.56 ± 0.13) × (ionization potential (eV)).

Finally, it must be noted that the computational effort in calculating ionization potentials is slightly less than that for bond strengths, and thus it should be the preferred tool for the generation of sufficiently accurate structure−reactivity empirical expressions.

3.7. Atmospheric Implications. The rate coefficients of several fluorinated alcohols with hydroxyl radicals and chlorine atoms are significantly higher than those for the most common hydrofluorocarbons as shown in Table 5. Approximate tropospheric lifetimes τ_{eff} were derived by assuming that an organic compound is removed from the atmosphere via its chemical reactions with OH and Cl with lifetimes τ_{OH} and τ_{Cl}, respectively

$$1/\tau_{eff} = 1/\tau_{OH} + 1/\tau_{Cl}$$

where $\tau_{OH} = 1/k_{OH}[OH]$ and $\tau_{Cl} = 1/k_{Cl}[Cl]$. The room-temperature rate coefficients k_{OH} and k_{Cl} were considered along with a spatially uniform diurnal global average for [OH] and [Cl] of 1×10^6 [36] and 1×10^4 molecule cm^{-3},[37,38] respectively. In particular, for larger alcohols, the Cl atom reactions contribute to about 20% of their total tropospheric removal. This indicates the importance of atmospheric oxidation processes initiated by chlorine atoms, especially in coastal areas, where Cl levels are established with increased confidence. Oxygenated HFCs are considered to be harmless to stratospheric ozone; therefore the presence of HFAs in the atmosphere may only slightly contribute to global warming. In addition, the presence of a hydroxyl group, apart from their tropospheric reactivity, also enhances their hydrophilicity compared to HFCs, which may further decrease their actual lifetimes, allowing their diffusion into cloud droplets or adsorption onto atmospheric aerosols, speeding up their removal via wet or dry deposition. The tropospheric oxidation products for alcohols of the general type R_F-CH_2OH are the corresponding aldehydes $R_F-CH=O$, which, being sufficiently polar, may be also removed via wet or dry deposition or via further degradation by sunlight photolysis. Moreover, there is a debate whether long-chain (>8C) fluorotelomer alcohols pose a threat to the environment,[39,40] because they consist of a likely source for the potentially toxic perfluorinated carboxylic acids (PFCAs).

Acknowledgment. This work is part of the project "Impact of Fluorinated Alcohols and Ethers on the Environment" and has received support from the CEC Environment and Climate Program (through Contract No. ENVK2-1999-00099). It was also supported by the Greek Secretariat of Research and Technology within the project TROPOS (2005−2006). Computational work was partially supported by the "Excellence in the Research Institutes" Program, Action 3.3.1, which was funded by the Greek Ministry of Development. We thank Dr. D. Levi of DuPont de Nemours International for providing us with the Teflon FEP 121A aqueous dispersion.

Supporting Information Available: Optimized structural parameters of all species and their harmonic vibrational frequencies. This material is available free of charge via the Internet at http://pubs.acs.org.

References and Notes

(1) World Meteorological Organization. *Scientific Assesment of Ozone Depletion: 2002*; Global Ozone Research and Monitoring Project, Report No. 47; World Meteorological Organization: Geneva, Switzerland, 2003.

(2) Molina, M. J.; Rowland, F. S. *Nature* **1974**, *249*, 810.

(3) Wallington, T. J.; Schneider, W. F.; Sehested, J.; Nielsen, O. J. *J. Chem. Soc., Faraday Discuss.* **1995**, *100*, 55.

(4) *Tokutei Furon, Tokutei Furon Siyousakugen Manyuaru*; Fluorocarbon Manufacturers Association: Tokyo, Japan, 1990.

(5) Hurley, M. D.; Misner, J. A.; Ball, J. C.; Wallington, T. J.; Ellis, D. A.; Martin, J. W.; Mabury, S. A.; Andersen, M. P. S. *J. Phys. Chem. A* **2005**, *109*, 9816.
(6) Graedel, T. E.; Keene, W. C. *Global Biogeochem. Cycles* **1995**, *9*, 45.
(7) Singh, H. B.; Thakur, A. N.; Chen, Y. E.; Kanakidou, M., *Geophys. Res. Lett.* **1996**, *23*, 1529.
(8) Spicer, C. W.; Chapman, E. G.; Finlayson-Pitts, B. J.; Plastridge, R. A.; Hubbe, J. M.; Fast, J. D.; Berkowitz, C. M. *Nature* **1998**, *394*, 353.
(9) Finlayson-Pitts, B. J.; Pitts, J. N., Jr. *Science* **1997**, *276*, 1045.
(10) Tanaka, P. L.; Oldfield, S.; Neece, J. D.; Mullins, C. B.; Allen, D. T. *Environ. Sci. Technol.* **2000**, *34*, 4470.
(11) Kelly, T.; Bossoutrot, V.; Magneron, I.; Wirtz, K.; Treacy, J.; Mellouki, A.; Le Bras, G. *J. Phys. Chem. A* **2005**, *109*, 347.
(12) Hurley, M. D.; Misner, J. A.; Ball, J. C.; Wallington, T. J.; Ellis, D. A.; Martin, J. W.; Mabury, S. A.; Sulbaek Andersen, M. P. *J. Phys. Chem. A* **2005**, *109*, 9816.
(13) Hurley, M. D.; Wallington, T. J.; Sulbaek Andersen, M. P.; Ellis, D. A.; Martin, J. W.; Mabury, S. A. *J. Phys. Chem. A* **2004**, *108*, 1973.
(14) Papadimitriou, V. C.; Prosmitis, A. V.; Lazarou, Y. G.; Papagiannakopoulos, P. *J. Phys. Chem. A* **2003**, *107*, 3733.
(15) Lazarou, Y. G.; Michael, C.; Papagiannakopoulos, P. *J. Phys. Chem.* **1992**, *96*, 1705.
(16) Golden, D. M.; Spokes, G. N.; Benson, S. W. *Angew. Chem., Int. Ed. Engl.* **1973**, *12*, 534.
(17) Sander, S. P.; Friedl, R. R.; Ravishankara, A. R.; Golden, D. M.; Kolb, C. E.; Kurylo, M. J.; Molina, M. J.; Moortgat, G. K.; Keller-Rudek, H.; Finlayson-Pitts, B. J.; Wine, P. H.; Huie, R. E.; Orkin, V. L. *Chemical Kinetics and Photochemical Data for Use in Atmospheric Studies, Evaluation Number 15*; JPL Publication 06-2; Jet Propulsion Laboratory, California Institute of Technology: Pasadena, CA, 2006.
(18) Frisch, M. J.; Trucks, G. W.; Schlegel, H. B.; Scuseria, G. E.; Robb, M. A.; Cheeseman, J. R.; Zakrzewski, V. G.; Petersson, G. A.; Montgomery, J. A., Jr.; Stratmann, R. E.; Burant, J. C.; Dapprich, S.; Millam, J. M.; Daniels, A. D.; Kudin, K. N.; Strain, M. C.; Farkas, O.; Tomasi, J.; Barone, V.; Cossi, M.; Cammi, R.; Mennucci, B.; Pomelli, C.; Adamo, C.; Clifford, S.; Ochterski, J.; Petersson, G. A.; Ayala, P. Y.; Cui, Q.; Morokuma, K.; Malick, D. K.; Rabuck, A. D.; Raghavachari, K.; Foresman, J. B.; Cioslowski, J.; Ortiz, J. V.; Stefanov, B. B.; Liu, G.; Liashenko, A.; Piskorz, P.; Komaroni, I.; Gomperts, R.; Martin, R. L.; Fox, D. J.; Keith, T. A.; Al-Laham, M. A.; Peng, C. Y.; Nanayakkara, A.; Gonzalez, C.; Challacombe, M.; Gill, P. M. W.; Johnson, B. G.; Chen, W.; Wong, M. W.; Andreas, J. L.; Head-Gordon, M.; Replogle, E. S.; Pople, J. A. *Gaussian 98*, revision A.7; Gaussian, Inc.: Pittsburgh, PA, 1998.
(19) Becke, A. D. *J. Chem. Phys.* **1993**, *98*, 5648.
(20) Perdew, J. P.; Burke, K.; Wang, Y. *Phys. Rev. B* **1996**, *54*, 16533.
(21) Lazarou, Y. G.; Prosmitis, A. V.; Papadimitriou, V. C.; Papagiannakopoulos, P. *J. Phys. Chem. A* **2001**, *105*, 6729.
(22) Papadimitriou, V. C.; Kambanis, K. G.; Lazarou, Y. G.; Papagiannakopoulos, P. *J. Phys. Chem. A* **2004**, *108*, 2666.
(23) Lee, C.; Yang, W.; Parr, R. G. *Phys. Rev. B* **1988**, *37*, 785.
(24) Perdew, J. P.; Chevary, J. A.; Vosko, S. H.; Jackson, K. A.; Pederson, M. R.; Singh, D. J.; Fiolhais, C. *Phys. Rev. B* **1992**, *46*, 6671.
(25) Curtiss, L. A.; Raghavachari, K.; Redfern, P. C.; Pople, J. A. *J. Chem. Phys.* **1998**, *109*, 42.
(26) McLean, A. D.; Chandler, G. S. *J. Chem. Phys.* **1980**, *72*, 5639.
(27) Frisch, M. J.; Pople, J. A.; Binkley, J. S. *J. Chem. Phys.* **1984**, *80*, 3265.
(28) Gill, P. M. W.; Johnson, B. G.; Pople, J. A.; Frisch, M. J. *Chem. Phys. Lett.* **1992**, *197*, 499.
(29) Dunning, T. H., Jr. *J. Chem. Phys.* **1989**, *90*, 1007.
(30) Dunning, T. H., Jr.; Peterson, K. A.; Wilson, A. K. *J. Chem. Phys.* **2001**, *114*, 9244.
(31) Chase, M. W. J. *J. Phys. Chem. Ref. Data* **1998**, (Monograph 9), 1.
(32) *NIST Chemistry WebBook*; NIST Standard Reference Database Number 69; National Institute of Standards and Technology: Gaithersburg, MD, June 2005. http://webbook.nist.gov/chemistry/.
(33) Evans, M. G.; Polanyi, M., *Trans. Faraday Soc.* **1938**, *34*, 11.
(34) Donahue, N. M. *Chem. Rev.* **2003**, *103*, 4593.
(35) Donahue, N. M.; Clarke, J. S.; Anderson, J. G. *J. Phys. Chem. A* **1998**, *102*, 3923.
(36) Kley, D. *Science* **1997**, *276*, 1043.
(37) Spicer, C. W.; Chapman, E. G.; Finlayson-Pitts, B. J.; Plastridge, R. A.; Hubbe, J. M.; Fast, J. D.; Berkowitz, C. M. *Nature* **1998**, *394*, 353.
(38) Pszenny, A. A. P.; Fischer, E. V.; Russo, R. S.; Sive, B. C.; Varner, R. K., *J. Geophys. Res., [Atmos.]* **2007**, *112*, D10S13 (DOI: 10.1029/2006JD007725).
(39) Ellis, D. A.; Martin, J. W.; Silva, A. O. D.; Mabury, S. A.; Hurley, M. D.; Andersen, M. P. S.; Wallington, T. J. *Environ. Sci. Technol.* **2004**, *38*, 3316.
(40) Wania, F. *Environ. Sci. Technol.* **2007**, *41*, 4529.
(41) Chen, J.; Young, V.; Niki, H.; Magid, H. *J. Phys. Chem. A* **1997**, *101*, 2648.
(42) Barry, J.; Locke, G.; Scollard, D.; Sidebottom, H. T., J.; Clerbaux, C.; Colin, R.; Franklin, J. *Int. J. Chem. Kinet.* **1997**, *29*, 607.
(43) Mogelberg, T. E.; Sehested, J.; Bilde, M.; Wallington, T. J.; Nielsen, O. J. *J. Phys. Chem.* **1996**, *100*, 8882.
(44) Rajakumar, B.; Burkholder, J. B.; Portmann, R. W.; Ravishankara, A. R. *Phys. Chem. Chem. Phys.* **2005**, *7*, 2498.
(45) Kovács, G.; Szász-Vadász, T.; Papadimitriou, V. C.; Dóbé, S.; Bérces, T.; Márta, F. *React. Kinet. Catal. Lett.* **2006**, *87*, 129.
(46) Tokuhashi, K.; Nagai, H.; Takahashi, A.; Kaise, M.; Sekiya, S. K. A.; Takahashi, M.; Gotoh, Y.; Suga, A. *J. Phys. Chem. A* **1999**, *103*, 2664.
(47) Chen, L.; Tokuhashi, K.; Kutsuna, S.; Sekiya, A.; Yonei, Y.; Yamamoto, A. *Chem. Phys. Lett.* **2003**, *382*, 277.